Diffusion Tensor Imaging of Peripheral Nerves: Current Status and New Developments

Daehyun Yoon, PhD[1] Amelie M. Lutz, MD[2]

[1] Department of Radiology and Biomedical Imaging, School of Medicine, University of California at San Francisco, San Francisco, California
[2] Department of Radiology, Kantonal Hospital Thurgau, Muensterlingen, Switzerland

Address for correspondence Amelie Lutz, MD, Department of Radiology, Kantonal Hospital Thurgau, Spital Campus 1, 8596 Muensterlingen, Switzerland (e-mail: amelie.lutz@team-radiologie.ch).

Semin Musculoskelet Radiol 2023;27:641–648.

Abstract

Diffusion tensor imaging (DTI) is an emerging technique for peripheral nerve imaging that can provide information about the microstructural organization and connectivity of these nerves and complement the information gained from anatomical magnetic resonance imaging (MRI) sequences. With DTI it is possible to reconstruct nerve pathways and visualize the three-dimensional trajectory of nerve fibers, as in nerve tractography. More importantly, DTI allows for quantitative evaluation of peripheral nerves by the calculation of several important parameters that offer insight into the functional status of a nerve. Thus DTI has a high potential to add value to the work-up of peripheral nerve pathologies, although it is more technically demanding. Peripheral nerves pose specific challenges to DTI due to their small diameter and DTI's spatial resolution, contrast, location, and inherent field inhomogeneities when imaging certain anatomical locations. Numerous efforts are underway to resolve these technical challenges and thus enable wider acceptance of DTI in peripheral nerve MRI.

Keywords
- diffusion tensor imaging
- peripheral nerve imaging
- magnetic resonance neurography

Diffusion tensor imaging (DTI) is an emerging technique in the work-up of peripheral nerve pathologies. As an extension of diffusion-weighted imaging (DWI), DTI is a specialized magnetic resonance imaging (MRI) technique that can provide information about the microstructural organization and connectivity of peripheral nerves and complement the information gained from anatomical non–nerve-specific sequences. It is particularly useful for examining the integrity and orientation of nerve fibers within a nerve.

DTI provides information about the orientation and connectivity of nerve fibers within a nerve bundle, further explained in this article. By analyzing diffusion tensor data, it is possible to reconstruct nerve pathways and visualize the three-dimensional (3D) trajectory of nerve fibers, as in nerve tractography. For example, this helps referring physicians understand the anatomical relationships and identify the specific nerve components involved in a tumor or injury. Studies suggest that tractography may be suitable to identify a "window" from which to approach the tumor resection preoperatively.[1]

More importantly, DTI allows for quantitative evaluation of peripheral nerves by calculating several important parameters. Fractional anisotropy (FA) exploits the fact that nerves have a very structured architecture with several intrinsic barriers composed of myelin, endoneurium, perineurium, and epineurium, facilitating water movement primarily along the long axis of the nerve and restricting free water diffusion along the short axis of nerves. Thus FA describes the physiologic anisotropy of nerves, and values range between 0 and 1, with healthy nerves demonstrating higher FA values and pathologic nerves having lower values. This reflects the normal close-to-directional diffusion in healthy nerves, and the abnormal, more isotropic diffusion in pathologic nerves.[2]

Issue Theme Molecular and Functional Imaging of Musculoskeletal Pain, Inflammation and Arthritis; Guest Editor, Sandip Biswal, MD

DOI https://doi.org/10.1055/s-0043-1775742.
ISSN 1089-7860.

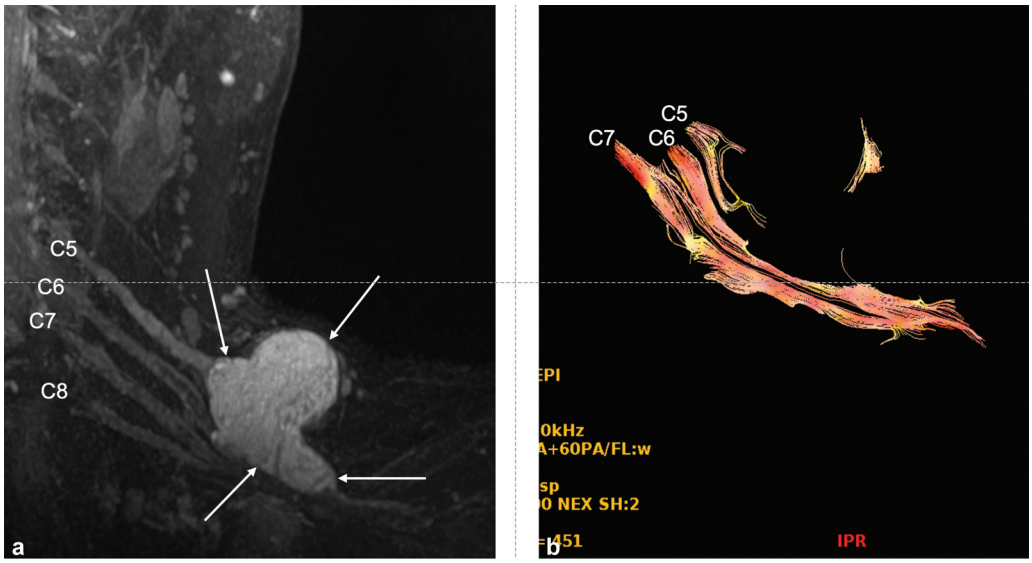

Fig. 1 Tractography in peripheral nerve sheath tumors. (**a**) Maximum intensity projection of a motion-sensitized driven-equilibrium Cube sequence in a 58-year-old patient with a hybrid peripheral nerve sheath tumor (schwannomatous and neurofibromatous differentiation) (arrows) of the left brachial plexus. (**b**) The tumor mainly involved C5, but partially also C6, and mainly displaces C7 on tractography images of those three nerves, derived from a multiplexed sensitivity encoding multi-shot echo planar imaging diffusion tensor imaging sequence, confirmed during surgery.

Mean diffusivity (MD) reflects the average of three diagonal eigenvectors of the diffusion tensor, used for apparent diffusion coefficient (ADC) maps.[3] By definition, MD is the average of (1) the direction of the largest eigenvector, axial diffusivity (AD), and (2) the average of the two smaller eigenvectors, expressed as radial diffusivity (RD). AD is considered a reflection of axonal integrity, whereas RD and FA reflect myelin sheath integrity.[4]

Defining normative values of FA, MD/ADC, RD, and AD is challenging due to considerable variability, even intra-individually or when comparing obtained FA and ADC values from the scanners of different vendors.[5] There is age-dependent variation in the FA: It tends to decrease with older age, maybe reflecting a decrease in the number of myelinated fibers in the peripheral nerves with advancing age.[4] There is also variation in absolute FA numbers between men and women, but the difference is negligible when corrected for body weight, because FAs are inversely associated with height, weight, and body mass index.[4] Similarly, an early study of FA and ADC values in median nerves found age- and location-dependent variation of the values.[6]

Using these principles, DTI has been used to evaluate nerve pathologies in trauma, tumors, inflammation, degeneration, and physiologic processes, such as nerve regeneration following nerve injury or surgical interventions. Changes in FA values, AD and RD, can indicate the progression or lack thereof in nerve healing. Any nerve injury causes a decrease in FA by disturbing fiber integrity and physiologic anisotropy of the involved nerve. This is caused by an increase in extracellular water and/or damage in the outer connective tissue layers of the nerve, depending on injury severity. Changes in RD provide additional information on the integrity of the nerve sheath structures. In contrast, increasing FA and decreasing RD values may suggest successful nerve regeneration, indicating recovery of the microstructural organization of the nerve fibers. A decrease in RD in regenerating nerves is considered most specific for successful regeneration, whereas persistently low FA and high RD may suggest the failure of a therapeutic approach.[7] Accordingly, in subclinical ulnar nerve neuropathy from a chronic injury, DTI was shown to be more sensitive than just relying on T2-weighted imaging alone.[8]

DTI can be particularly useful in evaluating peripheral nerve sheath tumors (PNSTs) by providing additional information about the tumor and its relationship with the surrounding nerves by localizing the tumor within/relative to the peripheral nerve and differentiating it from surrounding tissues (►**Fig. 1**). By analyzing the directionality of water diffusion, an analog to nerve microstructure, DTI can provide information about the microstructural organization of tumors and help characterize the tumor and understand its extent. It can aid in differentiating between an infiltrative (neurofibromas or invasive malignant PNSTs) and displacing nature (schwannoma) of a nerve sheath tumor.

Moreover, precise analysis of minimum diffusivity values (MD_{min}/ADC_{min}) can offer insight into the invasiveness of a PNST. It can be difficult to differentiate confidently between benign and malignant PNST by morphological criteria alone. Especially long-standing chronic (ancient) schwannomas present challenges. These tumors can be large and have complex features, including cystic degeneration and/or hemorrhagic areas that mimic features of malignant PNST. Low MD_{min}/ADC_{min} values correlate with higher cellularity of the tumor tissue, a common feature of malignant tumors. Tumor intrinsic MD_{min}/ADC_{min} values < 1 ($\times 10^{-3}$ mm^2/s) were shown to yield a specificity of 94% while maintaining a sensitivity of 100%, whereas fluorodeoxyglucose positron

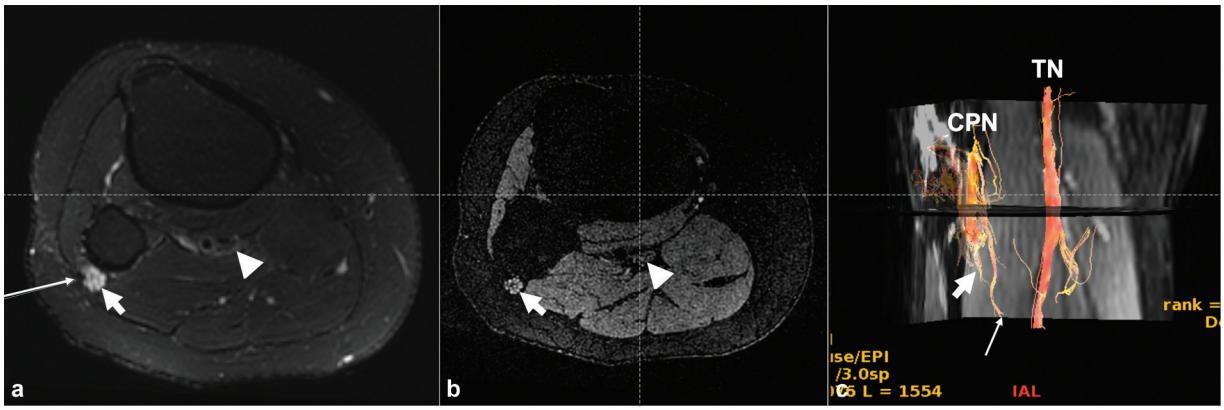

Fig. 2 Magnetic resonance neurography images of a 43-year-old patient, referred for the work-up of a suspected peripheral nerve sheath tumor of the right common peroneal nerve (CPN) detected on an outside magnetic resonance image. (**a**) Axial short tau inversion recovery image at the level of the tibial tuberosity of the right leg demonstrates an enlarged CPN (short arrow) at the fibular neck with mildly enlarged but markedly hyperintense fascicles. At close examination, it was noted that the myotendinous origin (long thin arrow) of the peroneus longus muscle was slightly more posterior reaching and more strongly developed than in most patients, causing long-standing impingement on the CPN at this level and subsequent moderate neuropathy. The normal tibial nerve (TN) is seen at the same level (arrowhead). (**b**) Second echo diffusion-weighted double-echo steady-state (DESS) image at the same level demonstrates the markedly signal-increased CPN (short arrow) as opposed to the normal TN (arrowhead), indicating neuropathic changes of the CPN. (**c**) Accordingly, tractography images derived from multiplexed sensitivity encoding multishot echo planar imaging diffusion tensor imaging demonstrated the enlarged CPN without disruption of fibers. Although the deep branch of the CPN (thin arrow) was easily followed in tractography, the superficial branch (short arrow) was more difficult to trace but appeared normal on images of the anatomical sequences.

emission tomography had a lower specificity of 83% when using a maximum standardized uptake value > 3.2.[9]

The imaging information on the potential functional impact and tumor histology that DTI can offer is important for treatment planning. It provides insights into the potential functional impact of the tumor on the nerve.[9,10] ►**Fig. 2** demonstrates an apparent peripheral nerve tumor case in which DTI helped prove a chronic impingement rather than neoplastic etiology of the nerve lesion.

DTI has been explored in numerous studies of patients with neuropathies including autoimmune-mediated, inherited, and systemic entities. To describe just two examples: In patients with demyelinating type 1 Charcot-Marie-Tooth disease, DTI of the sciatic nerves showed significant differences between healthy controls and patients, with decreased FA and increased MD, RD, and AD.[11] A case-control study exploring DTI in diabetic polyneuropathy showed that, as expected, there was a significant decrease in FA and an increase in ADC of both tibial and common peroneal nerves in diabetic polyneuropathy patients with an overall moderate, but significant correlation between DTI and nerve conduction studies. There was a significant positive correlation between FA and nerve conduction studies and a negative correlation between ADC and nerve conduction.[12]

When assessing patients with neuropathies or nerve injuries, it is currently still the norm to assess the physiologic status of the affected nerves with electrophysiologic examinations. Nerve conduction studies (NCS) and electromyography (EMG) help differentiate between demyelinating and axonal involvement.[13] In entities such as carpal tunnel syndrome, the diagnosis is typically made with NCS and EMG. Imaging, including MRI, used to be mainly employed in conjunction to determine the cause in atypical carpal tunnel cases, although it seems to have gained more popularity. There may be a certain lag time for electrophysiologic examinations to detect nerve injuries or changes in nerve regeneration. In addition, electrophysiologic studies are also more operator dependent than magnetic resonance neurography (MRN) with DTI.

Although larger scale studies are still needed to prove the value of DTI in the diagnostic work-up of peripheral nerve pathologies, MRN with DTI has a definite advantage over electrophysiologic examinations in the diagnostic work-up of plexuses that are in deeper body locations, and thus more challenging to access reliably for NCS, for example. A recent smaller scale study in patients with ulnar nerve neuropathy and healthy volunteers showed that T2 contrast-to-noise ratio in MRN and MD of DTI-based MRN delivered better results in depicting the precise site of ulnar nerve entrapment,[14] indicating added diagnostic value also in more superficially located nerves.

DTI even seems sensitive to subtle, transient nerve pathologies, such as in neurapraxia, causing measurable, albeit variable changes in peripheral nerves after compression with a tourniquet.[15] Similarly, changes induced by subtle stem cell therapy after a crush injury were detectable in experimental rat model studies. Animals undergoing stem cell therapy demonstrated measurably higher FA and lower RD in the treatment course, indicating therapy effects.[16]

Next, we discuss the physics of diffusion MRI, technical considerations, and new developments as potential solutions to the technical challenges of DTI.

Diffusion Magnetic Resonance Imaging Physics

Diffusion refers to the random motion of molecules resulting from their thermal energy, which is also called Brownian motion. The fundamental principles to sensitize MRI signals to the diffusion of water molecules were presented by a group of works in the 1980s.[17,18] This early nuclear magnetic

resonance research showed that the diffusion of water molecules leads to the nonzero phase accumulation on the water spins when a bipolar gradient waveform is applied. This phase incoherence of spins results in the signal cancellation and decrease of the net signal.[19]

The random spatial displacement of water molecules by diffusion is usually modeled to follow a zero-mean Gaussian distribution. The water molecules with fast (or freer) diffusion have a wider Gaussian distribution function than those with slow (or more restricted) diffusion. Because molecules naturally displace farther as time passes, the variance of the Gaussian distribution normalized by the time period during which spins are dephased and rephased by diffusion encoding gradient waveforms is used to quantify the diffusion, or diffusion coefficient (in the unit of distance squared divided by time).

Diffusion Tensor Imaging

Diffusion of water molecules in the human body usually does not occur equally in all directions because the random molecular motion is bound by the surrounding tissue structures. DTI[20,21] accounts for this directional variation of diffusion, by modeling the diffusion with a 3D random Gaussian distribution. In the DTI signal model, diffusion is determined by a symmetrical 3×3 diffusion tensor matrix. The elements of the diffusion tensor matrix are determined by fitting MRI signal measurements with at least six noncollinear diffusion encoding gradient directions. Then, eigen decomposition of the fitted tensor matrix is conducted, where the resulting eigenvalues form the AD (largest eigenvalue) and the RD (mean of the other two eigenvalues), and corresponding eigenvectors indicate the associated diffusion directions. FA and MD are secondary measures of diffusion derived from the eigenvalues to indicate the degree of diffusion anisotropy ($0 =$ isotropic; $1 =$ single directional diffusion) and the averaged diffusion, respectively. The sensitivity of DTI to tissue microstructure has provided a pathway to probe tissue microstructures beyond the nominal spatial resolution in the acquired MRI images.

Diffusion Magnetic Resonance Imaging Pulse Sequence

The major workhorse MRI pulse sequence for diffusion-weighted contrast and quantitative diffusion coefficient mapping is the single-shot spin echo diffusion-weighted echo planar imaging (DW-EPI) sequence. The DW-EPI sequence has been used for many different body parts, but its application to peripheral nerves has not yet been widely accepted. In essence, the many challenges of DW-EPI for peripheral nerves are because these nerves are quite small, whereas DW-EPI images have a coarse resolution, low signal-to-noise ratio (SNR), and are fraught with distortions. The following section introduces technical considerations about sequence parameter tuning and additional techniques for DW-EPI of peripheral nerves.

Receive Coil Selection

DWI/DTI from the DW-EPI sequence typically suffer from poor SNR, and therefore any measure to compensate for the low SNR without a substantial increase in scan time should be adopted. Thus the choice of the optimal receive coil for the target imaging volume is quite important because these coils can make a tremendous impact on SNR. A high-channel surface coil array closely fitting the imaging target body part is the best choice if available. Recently, major vendors released a large blanket-like flexible coil with a high number of coil elements (GE: AIR Coils; Siemens: Contour Coils). It has good potential to improve SNR of the brachial plexus where customized surface coil arrays have not been widely available.

Fat Suppression

Single-shot EPI is highly susceptible to off-resonance-induced distortion artifacts along the phase encoding direction because the pixel bandwidth along the phase encoding direction is quite small compared with the resonance frequency of fat. As a result, fat appears to be largely displaced along the phase encoding direction, and thus fat signal should be suppressed to avoid a pileup of artifacts on water signals. The spectral saturation of fat is probably the simplest solution without a major impact on scan time, but it does not work well in the area with strong off-resonance, such as the neck or torso. If local shimming to mitigate the off resonance is insufficient, nulling the fat signal based on the inversion recovery using short tau inversion recovery can be adopted, although it also partly reduces the water signal, depending on the T1 relaxation time of tissues. Another solution for fat suppression is to adopt Dixon-based techniques[22] for running fat-water separation through postprocessing,[23,24] although current implementations require longer acquisition and reconstruction times.

The b-Value Selection

The reciprocal value of the diffusion coefficient of the target tissue is a good candidate for the b-value to detect small changes around the assumed diffusion coefficient. However, the SNR should also be considered to prevent the DWI/DTI from being dominated by noise. A wide range of b-values (400–1,400 s/mm^2) was reported for diffusion MRI of various peripheral nerves, and there is no consensus yet about the optimal b-value.[25,26] A few studies recommended 600 s/mm^2 for a reasonable balance between SNR and sensitivity.[2,25] A recent study by Foesleitner et al[27] reported the non-Gaussian behavior of diffusion-weighted signals when they measured them over 16 b-values ranging from 0 to 1,500 s/mm^2. Interestingly, non-Gaussianity appeared beyond b-values of 600 s/mm^2 in the axial diffusion direction while it did so for b-values of 800 s/mm^2 in the radial diffusion direction, which led to a recommendation of 700 s/mm^2 for the b-value. They also demonstrated that for higher b-values, the bi-exponential and kurtosis model better fit in the measurement than the conventional mono-exponential signal model. Further investigations are necessary to identify specific nerve diseases that can benefit from this high b-value kurtosis model.

Diffusion Encoding Direction Selection

The number of diffusion encoding directions is another design parameter. In brain imaging, the high angular

resolution in the axial and radial diffusion directions of the white matter tracts requires a large number of diffusion encoding directions. However, in peripheral nerve imaging, except for some pathologic cases such as nerve sheath tumors, the orientation of the nerves (or axial/radial diffusion directions of nerves) can also be identified using structural, non–diffusion-weighted images. Therefore, the number of diffusion encoding directions is rather considered for finding an acceptable balance between the scan time and conditioning (or accuracy) of diffusion coefficient estimation. As in the case of b-values, there is no agreement on the optimal number of diffusion encoding directions, but 15 to 20 were reported to be a good candidate.[2,28]

Off-resonance-induced Distortion Correction

There have been localized shimming approaches to correct for the center frequency offset and linear component of the off-resonance frequency pattern in a slice-by-slice manner. Real-time B0 inhomogeneity[29] correction applies a different center frequency for each slice after calibration measurements to correct for the global translation artifact and imperfect fat saturation due to the center frequency mismatch. Adjustment of linear shimming for individual slice locations, so-called dynamic shimming,[30] demonstrated the improvement of off-resonance correction in body diffusion MRI.[31,32] High-order shimming[33] to correct for beyond zeroth (constant offset) and first-order (linear) components of the off-resonance pattern has been well adopted in brain diffusion MRI, but it has not yet been thoroughly investigated in body diffusion MRI or peripheral nerve diffusion MRI.

Off-resonance-induced signal translation in one spatial direction is proportional to the ratio of the off-resonance frequency over the pixel bandwidth determined by the encoding gradient amplitude in the direction. In single-shot EPI, the pixel bandwidth along the frequency encoding gradient direction is usually larger than the off-resonance frequency, and thus associated signal translation is insubstantial. The pixel bandwidth along the phase encoding direction, proportional to phase encoding step size over echo spacing, is usually much smaller than the off-resonance frequency, resulting in significant signal translation artifacts along the phase encoding direction. Therefore, pulse sequence techniques for off-resonance correction in DW-EPI have attempted to increase the phase encoding step size and/or decrease the echo spacing.

Readout-segmented EPI[34] decreases the echo spacing by using a reduced frequency field of view (FOV) that consequently needs shorter frequency encoding. A tailored radiofrequency (RF) pulse to excite signals selectively in both slice and phase directions can allow encoding a reduced phase FOV, which increases the phase encoding step size and reduces the off-resonance artifact.[35] Parallel imaging[36,37] facilitates undersampling along the phase encoding direction, which leads to the increased phase encoding step size and thus achieves a reduction of signal translation artifacts in addition to the accelerated scan time. ►**Fig. 3** shows a coronal DW-EPI image of the lumbosacral plexus where the combination of reduced phase FOV and parallel imaging further mitigated the off-resonance-induced distortion. Development of techniques to resolve shot-to-shot phase incoherence[38] enabled the use of multi-shot EPI for DW-EPI instead of single-shot EPI, where each shot acquires a segment of EPI undersampled along the phase encoding direction and as a result, mitigates the associated signal translation artifacts.

Numerous postprocessing methods have been developed for off-resonance artifact correction of EPI images. Reverse polarity gradient acquisition[39] is arguably one of the most popular methods and has been applied for DW-EPI of a wide range of body parts.[40–42] The method compares the two non–

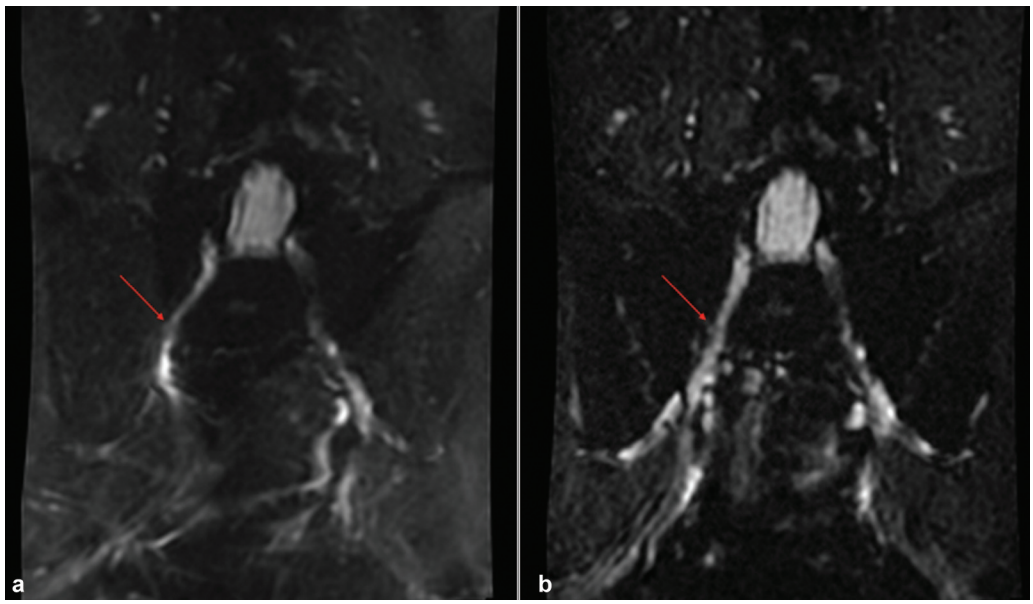

Fig. 3 Effects of parallel imaging on single-shot diffusion-weighted echo planar imaging (DW-EPI). (**a**) Coronal single-shot DW-EPI with reduced field of view (FOV). (**b**) Reduced FOV plus parallel imaging. The spatial distortion due to off resonance (red arrows) is further reduced by combining the two techniques.

diffusion-weighted (b0) EPI images, each acquired with an opposite polarity of the phase-encode gradient and then estimates the off-resonance frequency for each voxel, exploiting that signal translation occurs in the opposite direction between two compared images. The estimated off-resonance map is later used to undo the distortion of subsequentially acquired diffusion-weighted EPI images, assuming there is no major change in the underlying off-resonance pattern. The calibration scan with reverse polarity is usually simple to configure in the MRI scanner. The method works on the image domain requiring no raw k-space data and is supported by a major postprocessing tool (FSL software).[43]

Denoising

Denoising is probably one of the most well-accepted applications of machine learning, and the limited SNR issue of diffusion MRI makes it a very suitable application. A group of reports has been published using various training approaches for denoising DTI,[44] accelerated multi-shot DWI,[45] and multi b-value DTI.[46] As in the cases of many machine learning techniques, validation with disease cases should follow to establish the techniques in routine clinics.

Non–Diffusion-weighted Echo Planar Imaging Sequences

There have been developments of non–DW-EPI sequences for acquiring diffusion-weighted images that attempt to overcome the limited image quality by EPI. Using a single-shot or multi-shot fast spin-echo readout instead of an EPI readout[47] has demonstrated promise in achieving improved image sharpness with almost no distortion in imaging of various body parts.[48–50]

The major challenge with fast spin-echo readout approaches is that the bulk phase incoherence due to motion during diffusion encoding can cause instability in the readout fast spin-echo train, resulting in severe signal loss artifacts. Diffusion-weighted magnitude preparation schemes adopted a stabilizer gradient[48] to create a linear phase across the voxel to override a motion-induced phase offset, and it achieved decent image qualities. However, the linear phase by stabilizer also causes global attenuation of signal amplitude, and residual phase errors can result in quantification errors in diffusion estimates. The extra collection of phase navigators was suggested to account for the residual phase during the reconstruction of multi-shot FSE data demonstrated improved image quality in diffusion imaging of the lumbosacral plexus.[51]

Steady-state sequences, such as reverse fast imaging with steady-state free precession (PSIF) or double-echo steady state (DESS), can be configured to develop diffusion contrast[52,53] and run ADC mapping.[54] With steady-state sequences, it is rather difficult to implement strong diffusion-weighting corresponding to high b-values ($> 800\,s/mm^2$) in DW-EPI. However, steady-state sequence images are almost artifact-free in high spatial resolution, making them an attractive alternative to DW-EPI in running diffusion imaging of musculoskeletal tissue. This is because short T2/T2* relaxation times of musculoskeletal tissues cause severe blurring due to fast signal decay during EPI readout.

A high-resolution ADC mapping of human sciatic nerve fascicles in patients with Charcot-Marie-Tooth type 1A was recently presented using DESS at 7-T MRI.[55] The in-plane resolution was 0.15 mm $\times$ 0.15 mm with a slice thickness of 2 mm, significantly higher than the typical spatial resolution adopted in DW-EPI of peripheral nerves ($>$ 1 mm for in-plane, $\sim$ 3 mm for slice thickness). The diffusion sensitivity of the steady-state sequence also develops high susceptibility to motion artifacts. Therefore, further research on motion artifact suppression techniques for diffusion-weighted steady-state sequences, such as averaging phase incoherence by oversampling the central k-space,[56] should be followed for enabling robust diffusion mapping.

Conclusion

DTI will not likely replace electrophysiologic examinations in providing functional information on peripheral nerve status because EMG and NCS are tools that clinicians can perform themselves with easy access in the office setting. But DTI has a high potential to add value to and complement the work-up of peripheral nerve pathologies, although contrary to the already routine application in the central nervous system, DTI is more technically demanding in peripheral nerves. These nerves pose specific challenges to DTI due to their small diameter and DTI'S spatial resolution, similar contrast to neighboring veins and muscle, oftentimes off-isocenter location, and inherent field inhomogeneities when imaging (e.g., the brachial plexus). Nevertheless, DTI is increasingly entering the world of routine clinical MRN, and numerous efforts are underway to overcome the technical challenges of DTI and facilitate its transition to a mainstream imaging tool. In our experience, the demand is also very much driven by referring physicians because DTI can serve as a problem solver, especially in the work-up of mass lesions, in the posttraumatic and postsurgical setting. It may be beneficial to add DTI to clinical routine nerve imaging protocols in those settings.

Conflict of Interest
None declared.

References

1 Cage TA, Yuh EL, Hou SW, et al. Visualization of nerve fibers and their relationship to peripheral nerve tumors by diffusion tensor imaging. Neurosurg Focus 2015;39(03):E16
2 Jeon T, Fung MM, Koch KM, Tan ET, Sneag DB. Peripheral nerve diffusion tensor imaging: overview, pitfalls, and future directions. J Magn Reson Imaging 2018;47(05):1171–1189
3 O'Donnell LJ, Westin CF. An introduction to diffusion tensor image analysis. Neurosurg Clin N Am 2011;22(02):185–196, viii
4 Kronlage M, Schwehr V, Schwarz D, et al. Peripheral nerve diffusion tensor imaging (DTI): normal values and demographic determinants in a cohort of 60 healthy individuals. Eur Radiol 2018;28(05):1801–1808
5 Guggenberger R, Nanz D, Bussmann L, et al. Diffusion tensor imaging of the median nerve at 3.0 T using different MR scanners:

agreement of FA and ADC measurements. Eur J Radiol 2013;82 (10):e590–e596
6 Guggenberger R, Markovic D, Eppenberger P, et al. Assessment of median nerve with MR neurography by using diffusion-tensor imaging: normative and pathologic diffusion values. Radiology 2012;265(01):194–203
7 Martín Noguerol T, Barousse R, Gómez Cabrera M, Socolovsky M, Bencardino JT, Luna A. Functional MR neurography in evaluation of peripheral nerve trauma and postsurgical assessment. Radiographics 2019;39(02):427–446
8 Bäumer P, Pham M, Ruetters M, et al. Peripheral neuropathy: detection with diffusion-tensor imaging. Radiology 2014;273 (01):185–193
9 Ahlawat S, Blakeley JO, Rodriguez FJ, Fayad LM. Imaging biomarkers for malignant peripheral nerve sheath tumors in neurofibromatosis type 1. Neurology 2019;93(11):e1076–e1084
10 Mazal AT, Ashikyan O, Cheng J, Le LQ, Chhabra A. Diffusion-weighted imaging and diffusion tensor imaging as adjuncts to conventional MRI for the diagnosis and management of peripheral nerve sheath tumors: current perspectives and future directions. Eur Radiol 2019;29(08):4123–4132
11 Kim HS, Yoon YC, Choi BO, Jin W, Cha JG, Kim JH. Diffusion tensor imaging of the sciatic nerve in Charcot-Marie-Tooth disease type I patients: a prospective case-control study. Eur Radiol 2019;29 (06):3241–3252
12 Wu C, Wang G, Zhao Y, et al. Assessment of tibial and common peroneal nerves in diabetic peripheral neuropathy by diffusion tensor imaging: a case control study. Eur Radiol 2017;27(08): 3523–3531
13 Chung T, Prasad K, Lloyd TE. Peripheral neuropathy: clinical and electrophysiological considerations. Neuroimaging Clin N Am 2014;24(01):49–65
14 Ho MJ, Held U, Steigmiller K, et al. Comparison of electrodiagnosis, neurosonography and MR neurography in localization of ulnar neuropathy at the elbow. J Neuroradiol 2022;49(01):9–16
15 Breitenseher J, Jengojan SA, Kovar F, Prayer D, Kasprian G Mapping of transient peripheral nerve compression by 3 Tesla DTI (C-226). Poster presented at: European Society of Radiology; March 6–10, 2014; Vienna, Austria
16 Chen YY, Zhang X, Lin XF, et al. DTI metrics can be used as biomarkers to determine the therapeutic effect of stem cells in acute peripheral nerve injury. J Magn Reson Imaging 2017;45 (03):855–862
17 Le Bihan D, Breton E. Imagerie de diffusion in vivo par resonance magnetique nucleaire. CR Acad Sci Paris 1985;301:1109–1112
18 Taylor DG, Bushell MC. The spatial mapping of translational diffusion coefficients by the NMR imaging technique. Phys Med Biol 1985;30(04):345–349
19 Stejskal EO, Tanner JE. Spin diffusion measurements: spin echoes in the presence of a time-dependent field gradient. J Chem Phys 1965;42:288–292
20 Basser PJ, Mattiello J, LeBihan D. Estimation of the effective self-diffusion tensor from the NMR spin echo. J Magn Reson B 1994; 103(03):247–254
21 Pierpaoli C, Jezzard P, Basser PJ, Barnett A, Di Chiro G. Diffusion tensor MR imaging of the human brain. Radiology 1996;201(03): 637–648
22 Dixon WT. Simple proton spectroscopic imaging. Radiology 1984; 153(01):189–194
23 Hu Z, Wang Y, Dong Z, Guo H. Water/fat separation for distortion-free EPI with point spread function encoding. Magn Reson Med 2019;82(01):251–262
24 Dong Y, Koolstra K, Riedel M, van Osch MJP, Börnert P. Regularized joint water-fat separation with B_0 map estimation in image space for 2D-navigated interleaved EPI based diffusion MRI. Magn Reson Med 2021;86(06):3034–3051
25 Bruno F, Arrigoni F, Mariani S, et al. Application of diffusion tensor imaging (DTI) and MR-tractography in the evaluation of peripheral nerve tumours: state of the art and review of the literature. Acta Biomed 2019;90(5-S):68–76
26 Eppenberger P, Andreisek G, Chhabra A. Magnetic resonance neurography: diffusion tensor imaging and future directions. Neuroimaging Clin N Am 2014;24(01):245–256
27 Foesleitner O, Sulaj A, Sturm V, et al. Diffusion MRI in peripheral nerves: optimized *b* values and the role of non-Gaussian diffusion. Radiology 2022;302(01):153–161
28 Chianca V, Albano D, Messina C, et al. Diffusion tensor imaging in the musculoskeletal and peripheral nerve systems: from experimental to clinical applications. Eur Radiol Exp 2017;1(01):12
29 Fung MM, Wu G, Estkowski L, Xu D, Hinks S, Mayram E Realtime B0 inhomogeneity correction in multi-station diffusion imaging (1606). Paper presented at: Proceedings of the 23rd Annual Meeting of the International Society for Magnetic Resonance; May 30–June 5, 2015; Toronto, ON, Canada
30 Morrell G, Spielman D. Dynamic shimming for multi-slice magnetic resonance imaging. Magn Reson Med 1997;38(03):477–483
31 Qiu J, Liu J, Bi Z, et al. Integrated slice-specific dynamic shimming diffusion weighted imaging (DWI) for rectal cancer detection and characterization. Cancer Imaging 2021;21(01):32
32 McElroy S, Winfield JM, Westerland O, et al. Integrated slice-specific dynamic shimming for whole-body diffusion-weighted MR imaging at 1.5 T. Magn Reson Mater Biol Phys Med 2021;34 (04):513–521
33 Gruetter R. Automatic, localized in vivo adjustment of all first- and second-order shim coils. Magn Reson Med 1993;29(06): 804–811
34 Robson MD, Anderson AW, Gore JC. Diffusion-weighted multiple shot echo planar imaging of humans without navigation. Magn Reson Med 1997;38(01):82–88
35 Saritas EU, Cunningham CH, Lee JH, Han ET, Nishimura DG. DWI of the spinal cord with reduced FOV single-shot EPI. Magn Reson Med 2008;60(02):468–473
36 Pruessmann KP, Weiger M, Scheidegger MB, Boesiger P. SENSE: sensitivity encoding for fast MRI. Magn Reson Med 1999;42(05): 952–962
37 Griswold MA, Jakob PM, Heidemann RM, et al. Generalized autocalibrating partially parallel acquisitions (GRAPPA). Magn Reson Med 2002;47(06):1202–1210
38 Chen NK, Guidon A, Chang HC, Song AW. A robust multi-shot scan strategy for high-resolution diffusion weighted MRI enabled by multiplexed sensitivity-encoding (MUSE). Neuroimage 2013; 72:41–47
39 Holland D, Kuperman JM, Dale AM. Efficient correction of inhomogeneous static magnetic field-induced distortion in echo planar imaging. Neuroimage 2010;50(01):175–183
40 Rakow-Penner RA, White NS, Margolis DJA, et al. Prostate diffusion imaging with distortion correction. Magn Reson Imaging 2015;33(09):1178–1181
41 Teruel JR, Fjøsne HE, Østlie A, et al. Inhomogeneous static magnetic field-induced distortion correction applied to diffusion weighted MRI of the breast at 3T. Magn Reson Med 2015;74 (04):1138–1144
42 Treiber JM, White NS, Steed TC, et al. Characterization and correction of geometric distortions in 814 diffusion weighted images. PLoS One 2016;11(03):e0152472
43 Smith SM, Jenkinson M, Woolrich MW, et al. Advances in functional and structural MR image analysis and implementation as FSL. Neuroimage 2004;23(Suppl 1):S208–S219
44 Sagawa H, Fushimi Y, Nakajima S, et al. Deep learning-based noise reduction for fast volume diffusion tensor imaging: assessing the noise reduction effect and reliability of diffusion metrics. Magn Reson Med Sci 2021;20(04):450–456
45 Mani M, Magnotta VA, Jacob M. qModeL: A plug-and-play model-based reconstruction for highly accelerated multi-shot diffusion MRI using learned priors. Magn Reson Med 2021;86 (02):835–851

46 Lin YC, Huang HM. Denoising of multi b-value diffusion-weighted MR images using deep image prior. Phys Med Biol 2020;65(10): 105003
47 Alsop DC. Phase insensitive preparation of single-shot RARE: application to diffusion imaging in humans. Magn Reson Med 1997;38(04):527–533
48 Zhang Q, Coolen BF, Versluis MJ, Strijkers GJ, Nederveen AJ. Diffusion-prepared stimulated-echo turbo spin echo (DPsti-TSE): an eddy current-insensitive sequence for three-dimensional high-resolution and undistorted diffusion-weighted imaging. NMR Biomed 2017;30(07):
49 Wang X, Zhang Z, Chen Q, Li J, Xian J. Effectiveness of 3 T PROPELLER DUO diffusion-weighted MRI in differentiating sinonasal lymphomas and carcinomas. Clin Radiol 2014;69(11): 1149–1156
50 Sakamoto J, Yoshino N, Okochi K, et al. Tissue characterization of head and neck lesions using diffusion-weighted MR imaging with SPLICE. Eur J Radiol 2009;69(02):260–268
51 Cervantes B, Van AT, Weidlich D, et al. Isotropic resolution diffusion tensor imaging of lumbosacral and sciatic nerves using a phase-corrected diffusion-prepared 3D turbo spin echo. Magn Reson Med 2018;80(02):609–618
52 Granlund KL, Staroswiecki E, Alley MT, Daniel BL, Hargreaves BA. High-resolution, three-dimensional diffusion-weighted breast imaging using DESS. Magn Reson Imaging 2014;32(04):330–341
53 Zhang Z, Meng Q, Chen Y, et al. 3-T imaging of the cranial nerves using three-dimensional reversed FISP with diffusion-weighted MR sequence. J Magn Reson Imaging 2008;27(03):454–458
54 Bieri O, Ganter C, Scheffler K. Quantitative in vivo diffusion imaging of cartilage using double echo steady-state free precession. Magn Reson Med 2012;68(03):720–729
55 Sveinsson B, Rowe OE, Stockmann JP, et al. Feasibility of simultaneous high-resolution anatomical and quantitative magnetic resonance imaging of sciatic nerves in patients with Charcot-Marie-Tooth type 1A (CMT1A) at 7T. Muscle Nerve 2022;66(02): 206–211
56 Moran CJ, Cheng JY, Sandino CM, et al. Diffusion-weighted double-echo steady-state with a three-dimensional cones trajectory for non-contrast-enhanced breast MRI. J Magn Reson Imaging 2021;53(05):1594–1605